www.czasopisma.pan.pl PAN POLSKA AKADEMIA NAUK www.journals.pan.pl

A R C H I V E S O F M E T A L L U R G Y A N D M A T E R I A L S

Volume 59 2014 Issue 4

DOI: 10.2478/amm-2014-0252

J. MIETTINEN*, K. LILOVA**, G. VASSILEV***

THERMODYNAMIC DESCRIPTION OF TERNARY Fe-B-X SYSTEMS. PART 3: Fe-B-Mn

OPIS TERMODYNAMICZNY TRÓJSKŁADNIKOWYCH UKŁADÓW Fe-B-X. CZĘŚĆ 3: Fe-B-Mn

A thermodynamic optimization of the ternary Fe-B-Mn system is presented. The thermodynamic parameters of the binary sub-systems, Fe-Mn, Fe-B and B-Mn, are taken from earlier assessments slightly modifying the B-Mn system description. The thermodynamic parameters of the Fe-B-Mn system are optimized in this study using literature experimental thermodynamic and phase equilibrium data. The solution phases of the system are described using the substitutional solution model and the borides are treated as stoichiometric or semi-stoichiometric phases of the $(A,B)_pC_q$ type described with the two-sublattice models.

Keywords: phase diagrams, thermodynamic modelling, Fe-based systems, Fe-B-X systems thermodynamic database, Fe-B-Mn system

Przedstawiono termodynamiczny opis trójskładnikowego układu Fe-B-Mn. Parametry termodynamiczne dwuskładnikowych stopów Fe-Mn, Fe-B i B-Mn zostały zaczerpnięte z wcześniejszych opracowań, przy tym opis układu B-Mn został nieznacznie zmodyfikowany. Parametry termodynamiczne dla układu Fe-B-Mn zostały zoptymalizowane w tej pracy w oparciu o eksperymentalne równowagi fazowe i dane termodynamiczne zaczerpnięte z literatury. Roztwory stałe w układzie Fe-B-Mn opisano przy użyciu modelu roztworu substytucyjnego, a borki traktowane są jako fazy stechiometryczne lub półstechiometryczne typu $(A,B)_pC_q$ opisane przy użyciu modelu dwu podsieci.

1. Introduction

We build upon our earlier work [1] related to the development of boron containing iron-based Fe-B-X database, where boron is treated as a substitutional component. The first two contributions (Fe-B-Cr [1] and Fe-B-Ni [2] thermodynamic descriptions) published earlier in this journal, are thereafter followed by the current ternary Fe-B-Mn description. The purpose is to develop a simple and compatible thermodynamic database for steels, which provides important and practical input data for thermodynamic-kinetic models simulating their solidification. The new Fe-B-Mn description can be applied in the modeling of solidification and grain structure formation in various steels [3, 4].

In this third paper, the first thermodynamic optimization of the Fe-B-Mn system is performed using experimental thermodynamic and phase equilibrium data from the literature as no earlier assessment was found. The binary thermodynamic data used for the Fe-B system is taken from [1], from Huang [5] for Fe-Mn system and from Sun et al. [6] for B-Mn system. Given that Sun et al. [6] treated B as an interstitial component in the bcc, fcc, cbcc and cub phases, their descriptions were remodeled in the current study.

2. Phases, modeling and data

Table 1 shows the phases and their modeling in the current Fe-B-Mn assessment. The solution phases (L, bcc, fcc, cbcc, cub, bet) are described using the substitutional solution model and the Fe-B compounds (Fe_2B and Fe_2B) with two sublattice models, allowing substitutional solubility of Fe and Mn.

TABLE 1
Phases and their modeling in the present Fe–B–Mn description

Phase	Modeling
Liquid (L)	(B,Fe,Mn), substitutional, RKM[a]
bcc_A2 (bcc)	(B,Fe,Mn), substitutional, RKM
fcc_A1 (fcc)	(B,Fe,Mn), substitutional, RKM
cbcc_A12 (cbcc)	(B,Fe,Mn), substitutional, RKM
cub_A13 (cub)	(B,Fe,Mn), substitutional, RKM
beta-rhombo-B (bet)	(B,Mn), substitutional, RKM
Fe_2B (extending to Mn_2B)	$(Fe,Mn)_2(B)$, sublattice, RKM
FeB (extending to MnB)	(Fe,Mn)(B), sublattice, RKM
Mn_2B	$(Mn)_2(B)$, stoichiometric
Mn_3B_4	$(Mn)_3(B)_4$, stoichiometric
MnB_2	$(Mn)(B)_2$, stoichiometric
MnB_4	$(Mn)(B)_4$, stoichiometric

[a] – Redlich-Kister-Muggianu (Gibbs excess energy model)

* AALTO UNIVERSITY, SCHOOL OF CHEMICAL TECHNOLOGY, ESPOO, FINLAND
** PETER A. ROCK THERMOCHEMISTRY LABORATORY, UNIVERSITY OF CALIFORNIA AT DAVIS, CA, USA
*** UNIVERSITY OF PLOVDIV, FACULTY OF CHEMISTRY, PLOVDIV, BULGARIA

The Mn-B compounds (Mn_2B, Mn_3B_4, MnB_2 and MnB_4) are treated as stoichiometric phases. In agreement with the experimental data [7-9] a complete mutual solubility was assumed between Fe_2B and Mn_2B, and between FeB and MnB. Detailed descriptions of the substitutional solution, sublattice models, and their parameters are available from Qiu [10].

Experimental studies of the Fe-B-Mn system up to 1992 have been reviewed by Raghavan [9]. Table 2 shows the experimental information selected in the current optimization of the Fe-B-Mn system.

TABLE 2

Experimental data applied in the optimization of the Fe-B-Mn system

Experimental data	Reference
Liquidus projection	[8]
Liquidus data for 5 isothermal sections, between 1410 and 1150°C	[8]
Isothermal section, at 800°C	[7]
Liquidus data for 6 vertical sections, at 1, 3.3, 4.7, 8.8, 12.5 and 16.3%B	[8], [11]
Enthalpy of mixing in liquid alloys, at 1557°C	[12]

3. Results

The thermodynamic description of the Fe-B-Mn system is presented in Table 3. The parameters marked with a reference code were taken from earlier assessments and those marked with O* were optimized in the current study using literature experimental data (Table 3).

TABLE 3

Thermodynamic description of the Fe-B-Mn system. Thermodynamic data of pure components are given by [11, 12] unless not shown in the table. Parameter values except for Tc and β are in J/mol. Tc and β are the Curie temperature (K) and the effective magnetic moment (magneton), of a phase, respectively

liquid (1 sublattice, sites: 1, constituents: B,Fe,Mn)	**Ref.**
$L^{L}_{B,Fe}$ = (-133438+33.946T) + (+7771)(x_B-x_{Fe}) + (+29739)(x_B-x_{Fe})^2	[15]
$L^{L}_{B,Mn}$ = (-134141-15.714T) + (+32025-21.766T)(x_B-x_{Mn}) + (+59907)(x_B-x_{Mn})^2+ (-8724)(x_B-x_{Mn})^3	[6]
$L^{L}_{Fe,Mn}$ = (-3950+0.489T) + (1145)(x_{Fe}-x_{Mn})	[5]
$L^{L}_{B,Fe,Mn}$ = (-170000+60T)x_B+ (+100000-60T)x_{Fe} + (+30000-60T)x_{Mn}	O*
bcc (1 sublattice, sites: 1, constituents: B,Fe,Mn)	
$^oG^{bcc}_B$ =$^oG^{bet}_B$+ (+43514-12.217T)	[14]
$L^{bcc}_{B,Fe}$ = (-50000+42T)	[1]
$L^{bcc}_{B,Mn}$ = (-50000)	O*
$L^{bcc}_{Fe,Mn}$ = (-2759+1.237T)	[5]
Tc^{bcc} = 1043x_{Fe}-580x_{Mn}+123$x_{Fe}x_{Mn}$	[5]
β^{bcc} = 2.22x_{Fe}-0.27x_{Mn}	[5]
fcc (1 sublattice, sites: 1, constituents: B,Fe,Mn)	
$^oG^{fcc}_B$ =$^oG^{bet}_B$+ (+50208-13.478T)	[14]
$L^{fcc}_{B,Fe}$ = (-66000+50T)	[1]
$L^{fcc}_{B,Mn}$ = (-50000)	O*
$L^{fcc}_{Fe,Mn}$ = (-7762+3.865T) + (-259)(x_{Fe}-x_{Mn})	[5]
Tc^{fcc} = -201x_{Fe}-1620x_{Mn}+$x_{Fe}x_{Mn}$(-2282-2068(x_{Fe}-x_{Mn}))	[5]
β^{fcc} = -2.1x_{Fe}-1.86x_{Mn}	[5]

cd. TABLE 3

cbcc (1 sublattice, sites: 1, constituents: B,Fe,Mn)	
$^oG^{cbcc}_B$ =$^oG^{bet}_B$+ (+50208-13.478T)	[14]
$L^{cbcc}_{Fe,Mn}$ = (-10184)	[5]
cub (1 sublattice, sites: 1, constituents: B,Fe,Mn)	
$^oG^{cub}_B$ =$^oG^{bet}_B$+ (+50208-13.478T)	[14]
$L^{cub}_{Fe,Mn}$ = (-11518+2.819T)	[5]
bet (1 sublattice, sites: 1, constituents: B,Mn)	
$^oG^{bet}_{Mn}$ =$^oG^{cbcc}_{Mn}$+ (+40)	[6]
$L^{bet}_{B,Mn}$ = (-49500-21T)	[6]
Fe_2B (Mn_2B) (2 sublattices, sites: 0.6667:0.3333, constituents: Fe,Mn:B)	
$^oG^{Fe2B}_{Fe:B}$ = 0.6667$^oG^{bcc}_{Fe}$+0.3333$^oG^{bet}_B$+ (-26261+3.466T)	[15]
$^oG^{Fe2B}_{Mn:B}$ = 0.6667$^oG^{cbcc}_{Mn}$+0.3333$^oG^{bet}_B$+ (-31700-6.48T)	[6]
$L^{Fe2B}_{Fe,Mn:B}$ = (-3000) + (+3000)(y_{Fe}-y_{Mn})	O*
FeB (MnB) (2 sublattices, sites: 0.5:0.5, constituents: Fe,Mn:B)	
$^oG^{FeB}_{Fe:B}$ = 0.5$^oG^{bcc}_{Fe}$+0.5$^oG^{bet}_B$+ (-35150+6T)	[1]
$^oG^{FeB}_{Mn:B}$ = 0.5$^oG^{cbcc}_{Mn}$+0.5$^oG^{bet}_B$+ (-35800-10T)	[6]
$L^{FeB}_{Fe,Mn:B}$ = (+11500-2T)	O*
Mn_2Bx (2 sublattices, sites: 0.6707:0.3293, constituents: Mn:B)	
$^oG^{Mn2Bx}_{Mn:B}$ = 0.6707$^oG^{cbcc}_{Mn}$+0.3293$^oG^{bet}_B$+ (-31652-6.17T)	[6]
Mn_3B_4 (2 sublattices, sites: 0.4286:0.5714, constituents: Mn:B)	
$^oG^{Mn34B}_{Mn:B}$ = 0.4286$^oG^{cbcc}_{Mn}$+ 0.5714$^oG^{bet}_B$+ (-38786-6.99T)	[6]
MnB_2 (2 sublattices, sites: 0.3333:0.6667, constituents: Mn:B)	
$^oG^{MnB2}_{Mn:B}$ = 0.3333$^oG^{cbcc}_{Mn}$+0.6667$^oG^{bet}_B$+ (-21100-12.556T)	[6]
MnB_4 (2 sublattices, sites: 0.2:0.8, constituents: Mn:B)	
$^oG^{MnB2}_{Mn:B}$ = 0.2$^oG^{cbcc}_{Mn}$+0.8$^oG^{bet}_B$+ (-17744-4.593T)	[6]

O* – Parameter optimized in this work.

The calculated results are compared with the original experimental data to verify the optimization. All calculations were carried out using the ThermoCalc software [16].

Figs. 1-3 show the calculated Fe-B [1], Fe-Mn [5] and B-Mn phase diagrams [6], respectively. A reasonable agreement with the experimental data is observed. It can be concluded that the current remodeling of the bcc, fcc, cbcc and cub phases do not result in noticeable changes in the respective calculated B-Mn phase diagram (Fig. 3). In addition, the calculated boron solubility in these phases remains very low and comparable to that of Sun et al. [6].

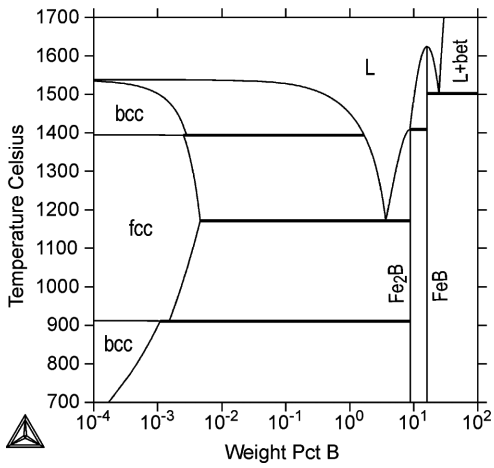

Fig. 1. Fe-B phase diagram calculated with the parameters of Miettinen and Vassilev [1]

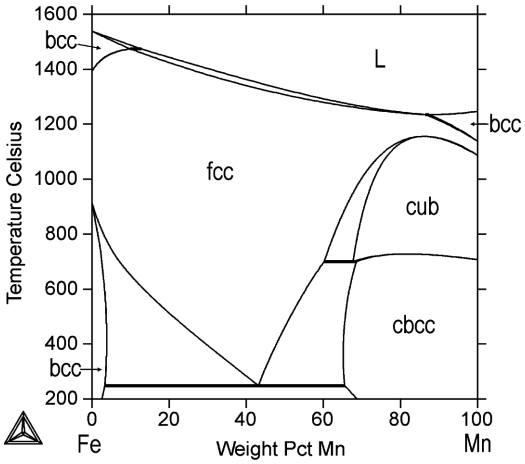

Fig. 2. Fe-Mn phase diagram calculated with the parameters of Huang [5]

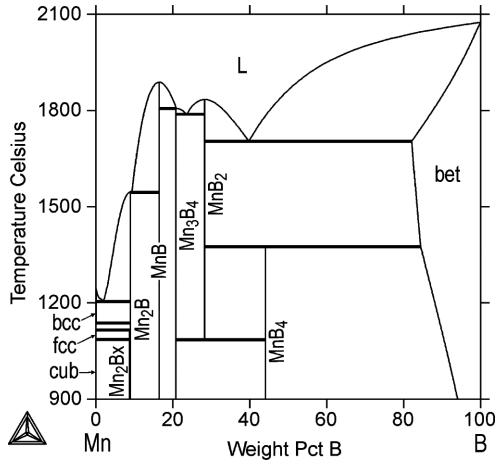

Fig. 3. B-Mn phase diagram calculated with the parameters obtained in this work, and those of Sun et al. [6]. No difference between both can be detected visually

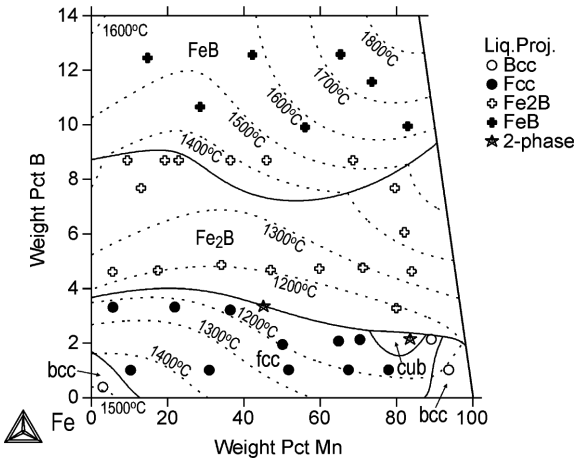

Fig. 4. Calculated liquidus projection of the Fe-B-Mn system, together with the experimental data points of Pradelli and Gianoglio [8]. Calculated liquidus isotherms between 1200 and 1800°C (dotted lines) are shown as well

The agreement between the calculated results for the Fe-B-Mn system and the experimental data (Table 2) is reasonable as shown in Figs. 4-16. The liquidus projection is shown in Fig. 4. One should be aware that the calculated primary FeB surface extends to B contents, which are lower than the presented experimental data. A small cub-phase region near the Mn corner appears. Such a monophase field has not been observed experimentally and the star symbols (Fig. 4) indicate the presence of two solid phases in the monovariant line. The lack of experimental evidences about the cub-phase region could be easily explained with the narrow range, thus additional investigations would be necessary to confirm or reject its existence in an equilibrium phase diagram.

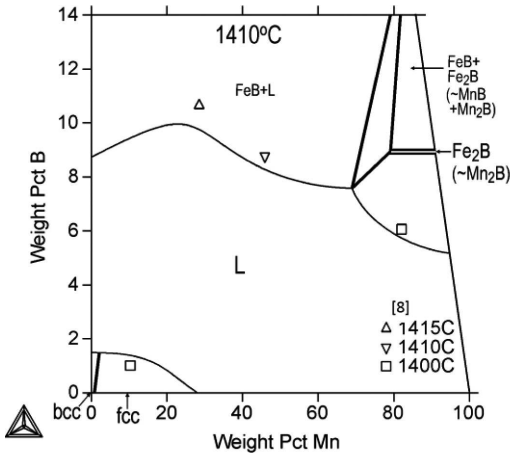

Fig. 5. Calculated isotherm of the Fe-B-Mn system at 1410°C, together with experimental data points [8]

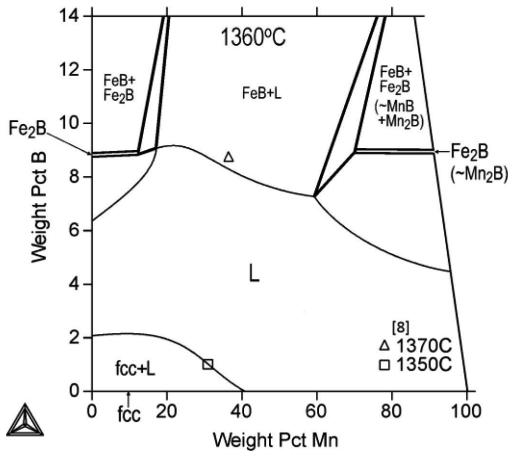

Fig. 6. Calculated isotherm of the Fe-B-Mn system at 1360°C, together with experimental data points [8]

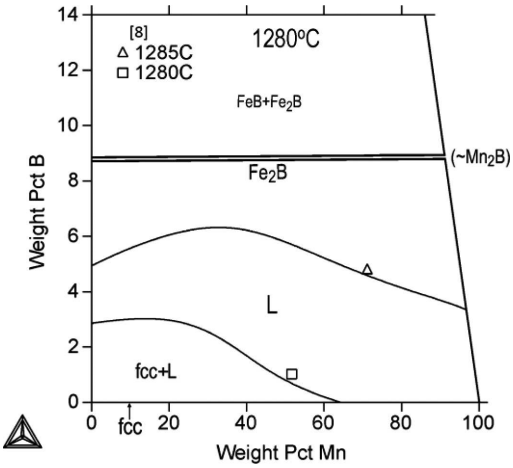

Fig. 7. Calculated isotherm of 1280°C in the Fe-B-Mn system, together with experimental data points [8]

Figures 5-10, and 11-14 show six isothermal and four vertical sections of the ternary system, respectively. According to the binary B-Mn description [6] used in this study, the MnB_2 and Mn_4B phases are not stable at 800°C (Fig. 10). The dotted line shows the calculated two-phase region of FeB+MnB_2 appearing if MnB_2 is modeled as a stable phase.

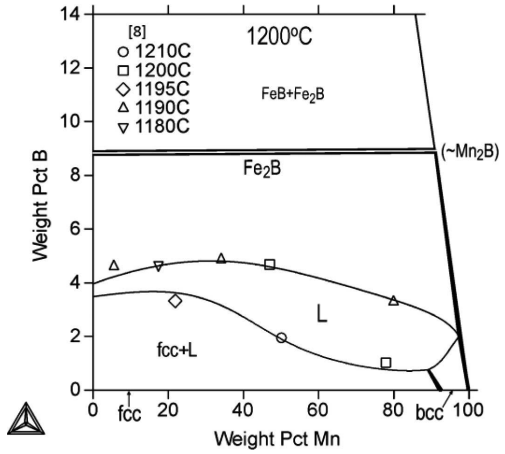

Fig. 8. Calculated isotherm of the Fe-B-Mn system at 1200°C, together with experimental data points [8]

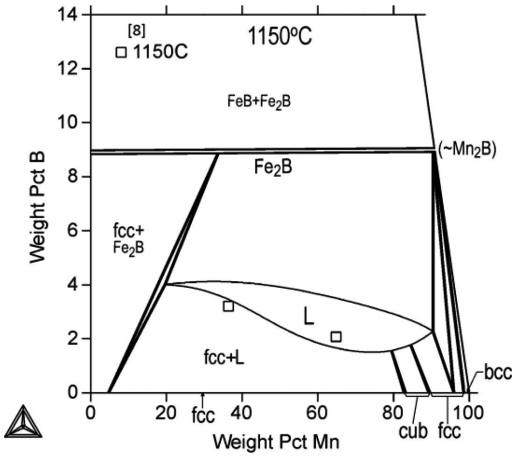

Fig. 9. Calculated isotherm of the Fe-B-Mn system at 1150°C, together with experimental data points [8]

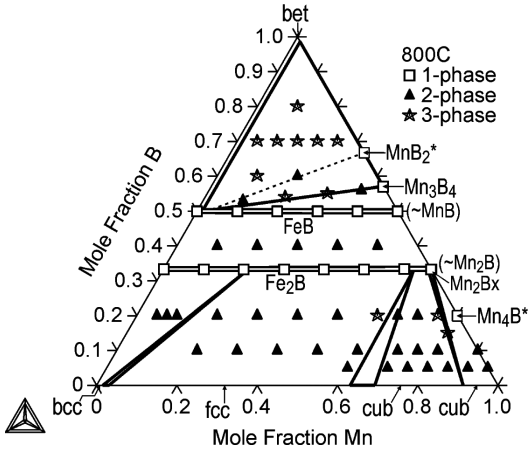

Fig. 10. Calculated isotherm of the Fe-B-Mn system at 800°C, together with experimental data points [7]. The phases marked by an asterisk are not stable at 800°C according to the original binary B-Mn description of Sun et al. [6]

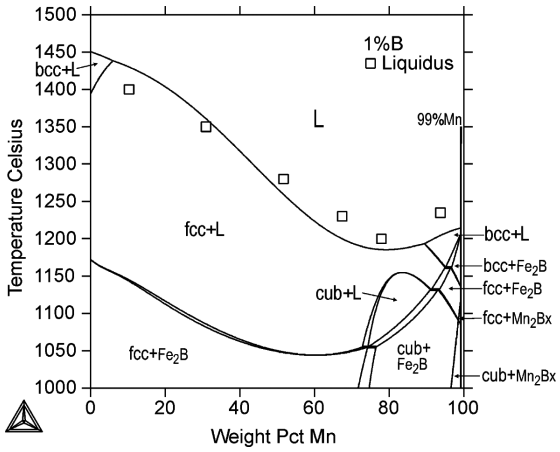

Fig. 11. Calculated vertical section of the Fe-B-Mn system at 1 wt% B, together with experimental liquidus points [8]

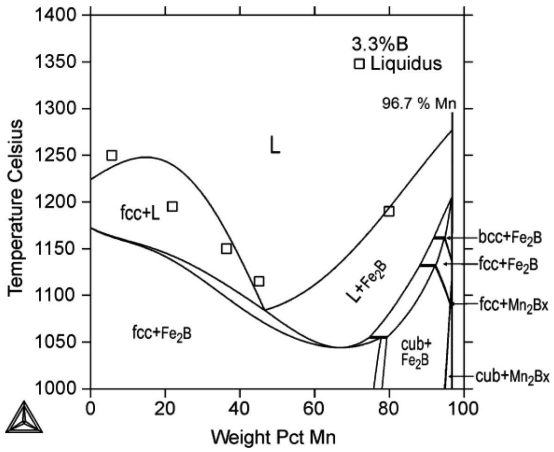

Fig. 12. Calculated vertical section of the Fe-B-Mn system at 3.3 wt% B, together with experimental data points [8]

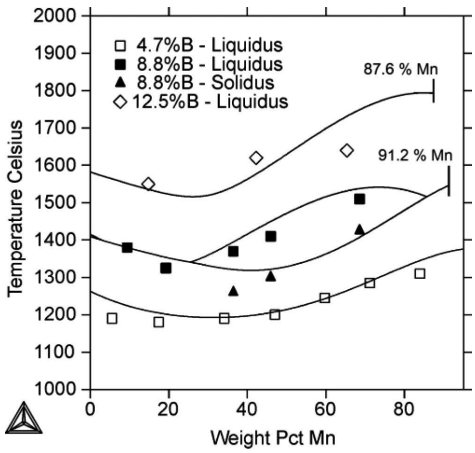

Fig. 13. Calculated vertical sections of the Fe-B-Mn system at 4.7, 8.8 and 12.5 wt% B, together with experimental data points [8]

The experimental topological data [11, 17-19] are compared with the calculated phase boundaries in a vertical section at 16.3 wt% B (Fig. 14).

The calculated ternary liquid alloys enthalpy of mixing at 1557°C is presented in Fig. 15 and a relatively good agreement with the experimental data of Witusiewicz [12] is observed.

Finally, Fig. 16 shows the calculated B solubility in the fcc phase. It can be concluded that the Mn content increase decreases the B content of the solid solutions. That boron

concentration is reduced also by the temperature drop from 1150 to 1000°C.

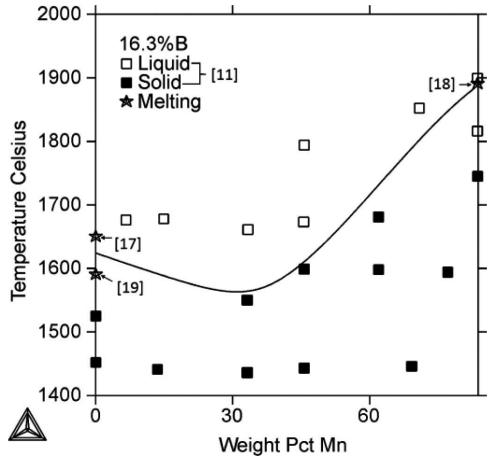

Fig. 14. Calculated vertical section of the Fe-B-Mn system at 16.3 wt% , together with experimental data points [11, 17-19]

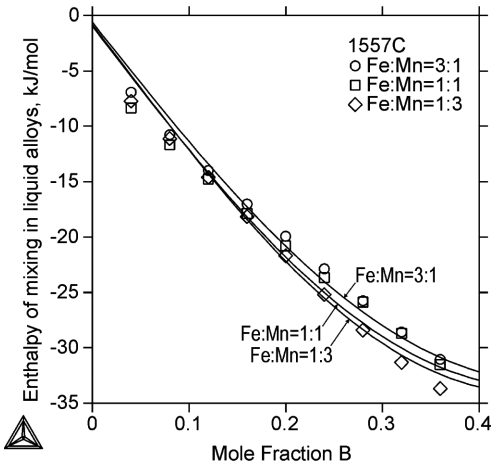

Fig. 15. Calculated molar enthalpy of mixing of liquid Fe-B-Mn alloys at 1557°C, together with experimental data points [12]. The reference states used are pure liquid components

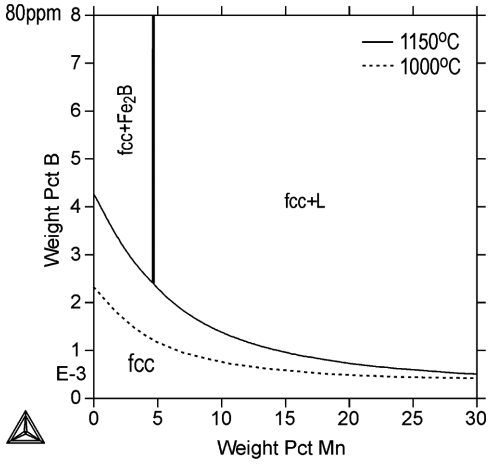

Fig. 16. Calculated B solubility in the fcc phase of the Fe-B-Mn system, at 1150 and 1000°C

4. Summary

A partial reoptimization of the B-Mn system is done. The present remodeling of the bcc, fcc, cbcc and cub phases does not result in noticeable changes of the calculated phase diagram. In addition, the calculated boron solubility in these phases remains very low.

Thereafter a thermodynamic optimization of the ternary Fe-B-Mn system is performed using the experimental thermodynamic and the phase equilibrium data from the literature. A complete mutual solubility was assumed between Fe_2B and Mn_2B, and between FeB and MnB. A good or reasonable agreement was obtained between the calculated and the experimental thermodynamic and phase equilibrium data.

Acknowledgements

Financial support of the Technology Development Centre (TEKES) during the Elemet Mocastro III project is gratefully acknowledged by Dr J Mietinen.

REFERENCES

[1] J. Miettinen, G. Vassilev, Thermodynamic description of ternary Fe-B-X systems. Part 1: Fe-B-Cr, submitted to Arch. Metall. Mater. **59**, 2 (2014) DOI:10.2478/amm-2014-0099
[2] J. Miettinen, G. Vassilev, Thermodynamic description of ternary Fe-B-X systems. Part 2: Fe-B-Ni, submitted to Arch. Metall. Mater. **59**, 2 (2014) DOI:10.2478/amm-2014-0100
[3] J. Miettinen, S. Louhenkilpi, H. Kytönen, J. Laine, Math. Comput. Simulat. **80**, 1536 (2010).
[4] A. Burbelko, J. Falkus, W. Kapturkiewicz, K. Solek, P. Drozdz, M. Wrobel, Arch. Metall. Mater. **57**, 379 (2012).
[5] W. Huang, CALPHAD **13**, 243 (1989).
[6] W. Sun, Y. Du, S. Liu, B. Huang, and C. Jiang, J. Phase Equilib. Diff. **31**, 357 (2010).
[7] Yu.B. Kuzma, M.V. Chepiga, and A.M. Plakhina, Inorg. Mater. **2**, 1038 (1966).
[8] G. Pradelli, and C. Gianoglio, Metall. Ital. **68**, 19 (1976).
[9] V. Raghavan, Phase Diagrams of Ternary Iron Alloys – Part 6A, Indian Institute of Metals, Calcutta, 358 (1992).
[10] C. Qiu, Thermodynamic study of carbon and nitrogen in stainless steels. Ph.D. Thesis, Royal Institute of Technology, Stockholm, 1993.
[11] T. Kanaizuka, J. Solid State Chem. **41**, 195 (1982).
[12] V.T. Witusiewicz, Thermochim. Acta **264**, 41 (1995).
[13] A.T. Dinsdale, SGTE unary database, version 4.4; www.sgte.org.
[14] I. Ansara, A.T. Dinsdale, and M.H. Rand, COST 507 – Thermochemical database for light metal alloys, Volume 2, European Communities, Belgium, 1998.
[15] B. Hallemans Wollants, and J.R. Roos, Z. Metallkd. **85**, 676 (1994).
[16] J-O. Andersson, T. Helander, L. Höglund, P. Shi, and B. Sundman, CALPHAD **26**, 273 (2002).
[17] K.I. Portnoi, M.Kh. Levinshkaya, and V.M. Romashov, Sov. Powder Metall. Met. Ceram. **8**, 657 (1969).
[18] P.L. Liao, and K.E. Spear, Bull. Alloy Phase Diagrams **7**, 543 (1986).
[19] F.A. Sidorenko, N.N. Serebrennikov, V.D. Budozhanov, Yu.V. Putintsev, S.N. Trushevskii, V.D. Korabanova V. Geld, High Temp. **15**, 36 (1977).

Received: 20 January 2014.